BMC Medical Imaging

RESEARCH

Open Access

Application of real-time shear wave elastography technology in healthy pediatric hip joints

Fan Xiangyang[1], Wang Ziwei[1], Zhou Jingjing[1], Di Min[1] and He Xiao[1*]

Abstract

Background Recently, pediatric hip joint diseases have received increasing attention, however, most researches focus on conventional ultrasound. The aim of our study is to explore the application of real-time shear wave elastography (SWE) technology in different tissue structures of healthy pediatric hip joints to distinguish between the normal and pathological states, and provide a normal reference range for shear wave Young's moduli for clinical practices and subsequent scientific researches.

Methods According to the selection criteria, 189 healthy full-term infants with 378 hip joints were enrolled, including 102 males and 87 females aged 2–90 days. They were divided into three groups based on age: 0–30 days (61 patients), 31–60 days (63 patients), and 61–90 days (65 patients). All the subjects underwent routine ultrasound examination to perform Graf typing, and then subjected to the SWE. The Young's moduli of the femoral head, acetabular lip, acetabular cartilage apex, gluteus medius, gluteus minimus, and iliacus were recorded. The differences in various parts among the three groups, between the left and right sides, and between males and females were compared. The 95% medical reference value range for each part was obtained and consistency test was conducted.

Results There was no statistically significant difference in various parts between the left and right hip joints ($P > 0.05$) or between males and females ($P > 0.05$). There were significant differences in the femoral head, acetabular lip, and acetabular cartilage apex among the three groups ($P < 0.05$). The Young's moduli of the femoral head, acetabular lip, and acetabular cartilage apex were positively correlated with age ($r_1 = 0.56$, $P < 0.05$; $r_2 = 0.51$, $P < 0.05$; $r_3 = 0.58$, $P < 0.05$). The Young's moduli of the gluteus medius, gluteus minimus, and iliacus were not correlated with age ($P > 0.05$). The intra- and inter-observer evaluation results both had a high correlation, and the 95% Confidence Interval (95% CI) of both were relatively concentrated.

Conclusion Real-time SWE technology can be used to obtain the Young's moduli of healthy pediatric hip joints and surrounding tissues, and distinguish between healthy and pathological states. This can provide a normal reference range for shear wave Young's moduli for clinical practices and subsequent scientific researches.

Keywords Elasticity imaging techniques, Hip joint, Hip dislocation, Congenital, Hardness

*Correspondence:
He Xiao
hx126cc@126.com
[1]The First Affiliated Hospital of Zhengzhou University, Zhengzhou 450003, China

Background

In recent years, pediatric hip diseases have received increasing attention from parents and clinicians all around the world, with Developmental Dysplasia of the Hip (DDH) being the most common. DDH is one of the major diseases leading to physical disability in children, and its incidence varies from 0.06/1000 to 76.1/1000 in different countries and regions [1–2]. DDH incidence is greater in female infants than in male infants [3].

Currently, the mainstream diagnostic methods are high-frequency ultrasound and X-ray. Newborns and infants are in the early stages of hip joint development. During this period, the femoral head and cartilage apex are not yet ossified and cannot be shown by X-ray, but these unossified tissues can be clearly shown on ultrasound images, providing the possibility of routine ultrasound and shear wave elastography (SWE) examinations. Moreover, high-frequency ultrasound has the advantages of real-time use and no radiation and can also fully display the internal structure of the hip joint. Ultrasound imaging for the diagnosis of pediatric hip disorders was proposed as early as 1980 by Professor Reinhard Graf and is widely used in developed countries. He classified DDH into types I-IV, which is by far the simplest and most useful ultrasound screening technique. At 3–6 months after birth, the ossification center of the femoral head gradually appears to produce acoustic shadows, and the accuracy of ultrasound decreases. However, as the ossification center expands, the acetabulum does not show up well on ultrasound, and X-ray can be used at this time, so high-frequency ultrasound has become the preferred method for the early diagnosis of DDH in the clinic. The latest consensus of the International Interdisciplinary Consensus DDH Evaluation Committee of 2019 showed that clinical examination of newborns can detect hip joint instability but not acetabular dysplasia, whereas ultrasound is more sensitive and specific for the diagnosis of DDH [4]. In 2023, the British Society of Pediatric Orthopedics advocated universal hip ultrasound in infants up to 3 months to screen for DDH [5]. In some countries, ultrasonography has even been used as the gold standard for the diagnosis of DDH [6], facilitating the development of a clinical therapeutic schedule and assessment of patient prognosis.

Conventional high-frequency ultrasound cannot assess the stiffness of the hip joint and surrounding tissues, whereas real-time shear wave elastography (SWE) can quantitatively reflect the degree of tissue stiffness and has the advantages of real-time, noninvasive, and good reproducibility. Currently, SWE is only applied in the adult hip joint and its surrounding muscles, and evaluations of the pediatric hip joint and its surrounding soft tissues and muscles have not been reported [7].

The aim of this study was to use SWE technology to reflect changes in the hardness of healthy hip joints and surrounding tissues in pediatric patients, obtain normal elasticity values, differentiate between the healthy and pathological states of the hip joints; to provide technical support for early diagnosis, surgical plan selection, and postoperative follow-up of clinical DDH; and to provide a normal reference range for subsequent scientific researches.

Patients and methods

Study cohort

This study was a retrospective study. From May 2023 to March 2024, the infant registration number was entered in the Picture Archiving and Communication System (PACS) of the First Affiliated Hospital of Zhengzhou University to select the infant to query its basic information and clinical signs. A total of 216 healthy full-term infants without abnormal indications were selected for hip joint ultrasound examination. After excluding 9 infants who were unable to cooperate with the examination due to crying, 5 infants with poor image quality, 6 infants who were not Graf I type, and 7 infants who were unable to obtain informed consent from their guardians, 189 infants (378 hips, 102 males and 87 females) aged 2–90 days were enrolled as the study cohort finally. The infants were divided into three groups according to age: 1–30 days (61 cases), 31–60 days (63 cases) and 61–90 days (65 cases).

The inclusion criterion:

Healthy full-term infants;

Infants who were classified as type I by the Graf method.

Graf type I was defined as an α angle greater than 60°. The α angle is the angle between the baseline of the external border of the ilium bone and the apex of the acetabular angle.

The exclusion criteria:

Infants who were obese or emaciated according to the NHMRC's Growth Standards for Children Under 7 Years of Age;

Infants who had hip diseases;

Infants who did not cooperate with the examination;

Infants whose images were unclear;

Infants who were unable to provide the informed consent.

The study was approved by the Institutional Ethics Committee (2023-KY-0335-002), and informed consent was signed by the guardians of all the subjects.

Instruments and methods

A GE LOGIQ E20 color Doppler ultrasound diagnostic instrument with a 6–15 MHz frequency probe (ML6–15) equipped with SWE function was used. All the subjects

lay on their sides in quiet state to fully expose the position of the hip joints, which should be in a slightly flexed position. The musculoskeletal mode was selected on the machine. After applying an appropriate amount of heated coupling agent on the probe, the probe was gently placed at the hip joint of the child for imaging. Preferably, the greater trochanter of the femur, the femoral neck and the acetabulum were in the same plane, the image was frozen after displaying the standard section. The α and β angles of the hip joint were measured to perform Graf typing. Then the probe was switched to SWE mode, placed gently on top of the coupling agent without applying pressure to it. The elastography sampling frame was adjusted to cover the entire hip joint as much as possible by adjusting the probe angle appropriately and adjusting the machine depth. After three excitations of shear waves, the elastography sampling frame was filled with color and no noise, and then the image was frozen. The elasticity values of the femoral head, acetabular lip, acetabular cartilage apex, gluteus medius, gluteus minimus, and iliacus of the hip joint were measured. Then the infant was changed to a supine position, the iliacus was imaged and its elasticity value was measured by the same method as above. A circular quantitative detection area was selected in the imaging area, with the diameter of the detection area of the femoral head being approximately 5 mm, the diameter of the detection area of the acetabular lip and acetabular cartilage apex being approximately 1 mm, and the diameter of the detection area of the gluteus medius, gluteus minimus and iliacus being approximately 2 mm. The Young's moduli were recorded. The hip joint on the opposite side was measured using the same method.

The above data were sampled at least three times from the same position, and the average value was taken as the final result. All of them were operated by two ultrasonographers in the pediatric group with more than 10 years of working experience. When there was any ambiguity between the two ultrasonographers regarding pediatric hip typing, the chief pediatric ultrasonographer was asked to interpret the data, which were taken as the final result (Fig. 1).

After one week, two doctors measured the above parameters twice using the same method, and the same doctor measured the above parameters using the same method in sequence for consistency testing.

Statistical analysis

SPSS 27.0 statistical analysis software was used, the normally distributed data are expressed as the means ± standard deviations ($\bar{x} \pm s$), the t test was used to compare the differences between two independent groups, the nonnormally distributed data are expressed as *M* (*Q1*, *Q3*), and the Mann–Whitney *U* test was used to compare two groups. One-way ANOVA was used for comparisons among three groups for normally distributed and variance-aligned measurement data, and the Kruskal–Wallis *H* test was used for comparisons among three groups for non-normally distributed measurement data. The 95% reference range for normally distributed measurement data was determined via the approximate normality method, and the 95% reference range for nonnormally distributed measurement data was determined via the percentile method. Correlations between groups were analyzed via Spearman correlation analysis. The intraclass correlation coefficients (ICCs) were calculated and the intra- and inter-observer repeatability tests were perfomed. And the differences were considered statistically significant at $P < 0.05$.

Results

General clinical data: A total of 189 subjects were included in this study, among whom 102 (53.96%) were male.

Comparisons between the left and right sides revealed that the differences in the femoral head, acetabular lip, acetabular cartilage apex, gluteus medius, gluteus minimus, and iliacus of the hip joint were not statistically significant ($P > 0.05$). The Young's moduli and the 95% medical reference value range of each part were as follows: femoral head (left 23.72 ± 4.46 kPa, 14.98–32.46 kPa; right 23.89 ± 4.41 kPa, 15.25–32.53 kPa), acetabular lip (left 33.63 ± 6.59 kPa, 21.30–46.55 kPa; right 33.07 ± 7.22 kPa, 18.92–47.22 kPa), acetabular cartilage apex (left 22.47 ± 4.30 kPa, 14.04–30.89 kPa; right 22.31 ± 4.23 kPa, 14.02–30.60 kPa), gluteus medius (left 12.09 (10.98–13.11) kPa, 7.89–20.80 kPa; right 11.87 (10.97, 12.95) kPa, 5.64–20.61 kPa), gluteus minimus (left 11.89 (10.33, 14.05) kPa, 7.74–24.91 kPa; right 12.39 (10.98, 14.39) kPa, 6.83–22.95 kPa) and iliacus (left 10.92 (9.29, 12.19) kPa, 5.26–17.79 kPa; right 10.98 (9.84, 12.34) kPa, 5.94–17.59 kPa) (Table 1).

Comparisons between genders revealed that the differences in the hip femoral head, acetabular lip, acetabular cartilage apex, gluteus medius, gluteus minimus and iliacus were not statistically significant ($P > 0.05$). The values of the Young's modulus and 95% medical reference range for each site were calculated as the average of the left and right values: femoral head (male 23.55 ± 4.62 kPa, 14.49–32.61 kPa; female 24.12 ± 4.18 kPa, 15.92–32.31 kPa), acetabular lip (male 33.29 ± 7.13 kPa, 19.32–47.26 kPa; female 33.41 ± 6.65 kPa, 20.38–46.44 kPa), acetabular cartilage apex (male 22.15 ± 4.54 kPa, 13.25–31.05 kPa; female 22.67 ± 3.90 kPa, 15.03–30.31 kPa), gluteus medius (male 11.91 (10.96, 13.27) kPa, 6.05–22.45 kPa; female 12.31 (10.98, 13.40) kPa, 9.01–19.82 kPa), gluteus minimus (male 12.04 (10.78, 14.32) kPa, 6.24–23.29 kPa; female 12.32 (10.92, 14.31) kPa, 8.10–23.37 kPa) and

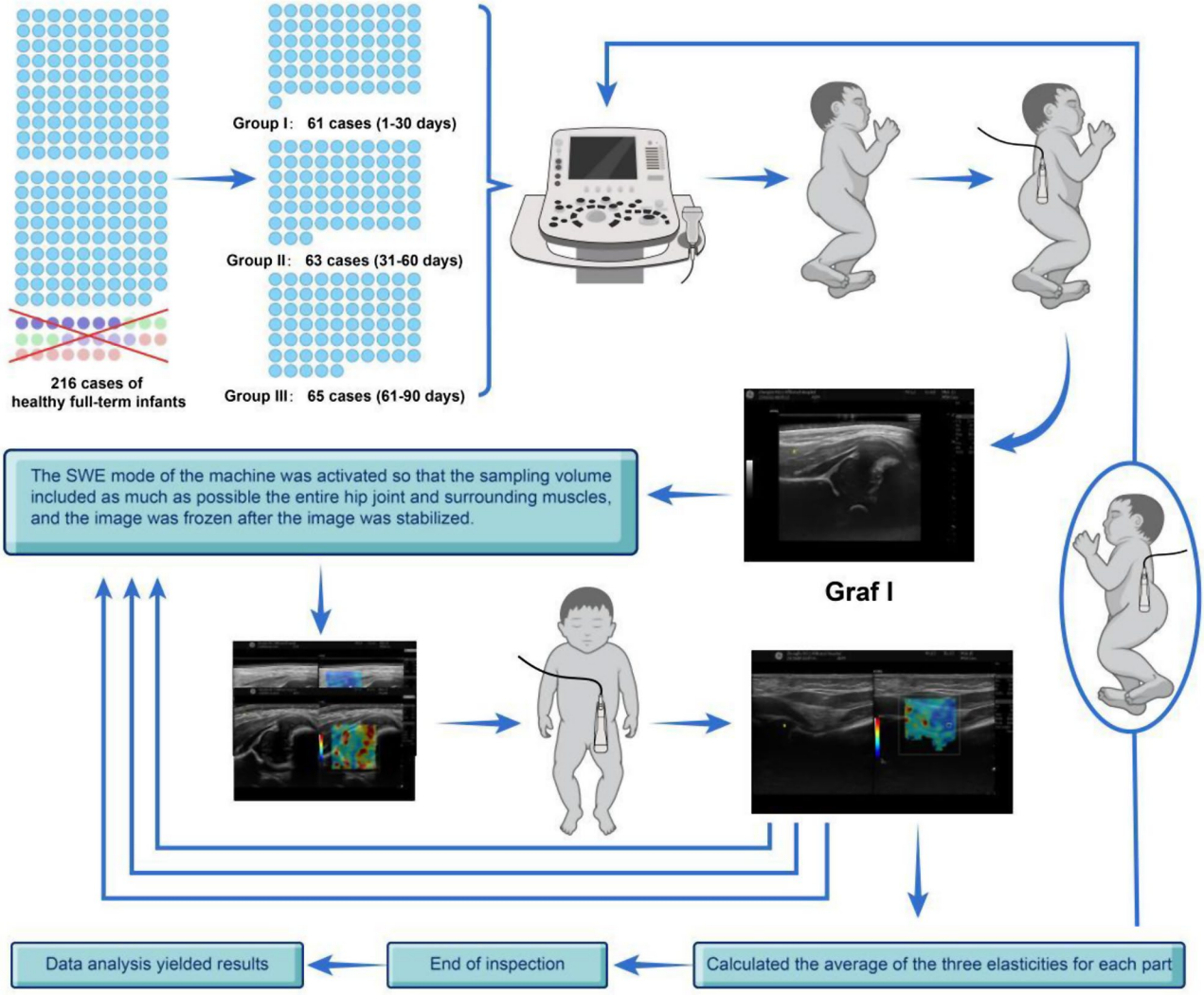

Fig. 1 Research flow chart

Table 1 Young's moduli of various parts of the hip joint and comparison results between the left and right sides (kPa)

Groups	Left		Right		t value/Z value	*P* value
	Young's moduli	95% medical reference value	Young's moduli	95% medical reference value		
Femoral head ()	23.72 ± 4.46	14.98–32.46	23.89 ± 4.41	15.25–32.53	-0.38 (*t* value)	>0.05
Acetabular lip ()	33.63 ± 6.59	21.30-46.55	33.07 ± 7.22	18.92–47.22	0.78 (*t* value)	>0.05
Acetabular cartilage apex ()	22.47 ± 4.30	14.04–30.89	22.31 ± 4.23	14.02–30.60	0.34 (*t* value)	>0.05
Gluteus medius *M(Q1, Q3)*	12.09(10.98, 13.11)	7.89–20.80	11.87(10.97, 12.95)	5.64–20.61	-0.84 (*Z* value)	>0.05
Gluteus minimus *M(Q1, Q3)*	11.89(10.33, 14.05)	7.74–24.91	12.39(10.98, 14.39)	6.83–22.95	-1.96 (*Z* value)	>0.05
Iliacus *M(Q1, Q3)*	10.92(9.29, 12.19)	5.26–17.79	10.98(9.84, 12.34)	5.94–17.59	-1.60 (*t* value)	>0.05

iliacus (male 10.92 (9.03, 12.15) kPa, 4.89–16.86 kPa; female 10.98 (9.87, 12.41) kPa, 6.08-17.67 kPa) (Table 2).

The differences among the three groups in the femoral head, acetabular lip and acetabular cartilage apex in the hip joint were statistically significant ($P<0.05$), and the differences in the gluteus medius, gluteus minimus and iliacus were not statistically significant ($P>0.05$). All the values of the Young's modulus and 95% medical reference range for each site were calculated as the average of the left and right values. (Table 3; Figs. 2, 3 and 4)

Correlation analysis: Young's moduli of the femoral head, acetabular lip and acetabular cartilage apex of the hip joint were positively correlated with age, and the values gradually increased with age ($r_1=0.56$, $P<0.05$; $r_2=0.51$, $P<0.05$; $r_3=0.58$, $P<0.05$). There was no

Table 2 Young's moduli of various parts of the hip joint and comparison results between males and females (kPa)

Groups	Male		Female		t value/Z value	*P* value
	Young's moduli	95% medical reference value	Young's moduli	95% medical reference value		
Femoral head ()	23.55 ± 4.62	14.49–32.61	24.12 ± 4.18	15.92–32.31	-1.26(*t* value)	>0.05
Acetabular lip ()	33.29 ± 7.13	19.32–47.26	33.41 ± 6.65	20.38–46.44	-1.56(*t* value)	>0.05
Acetabular cartilage apex ()	22.15 ± 4.54	13.25–31.05	22.67 ± 3.90	15.03–30.31	-1.19(*t* value)	>0.05
Gluteus medius *M(Q1, Q3)*	11.91(10.96,13.27)	6.05–22.45	12.31(10.98,13.40)	9.01–19.82	-0.73(*Z* value)	>0.05
Gluteus minimus *M(Q1, Q3)*	12.04(10.78,14.32)	6.24–23.29	12.32(10.92,14.31)	8.10-23.37	-1.01(*Z* value)	>0.05
Iliacus *M(Q1, Q3)*	10.92(9.03,12.15)	4.89–16.86	10.98(9.87,12.41)	6.08–17.67	-1.56(*Z* value)	>0.05

Table 3 Young's moduli of various parts of the hip joint and comparison results among the three groups (kPa)

Groups	1–30 days	31–60 days	61–90 days	F/H value	*P* value
Femoral head ()	20.36 ± 4.06	24.66 ± 3.75	26.23 ± 3.22	84.64(*F* value)	<0.05
Acetabular lip ()	29.21 ± 6.82	33.85 ± 5.79	36.75 ± 5.92	47.46(*F* value)	<0.05
Acetabular cartilage apex ()	19.29 ± 3.61	22.96 ± 3.84	24.75 ± 3.40	73.48(*F* value)	<0.05
Gluteus medius *M(Q1, Q3)*	11.91(10.96,12.96)	12.31(10.98,13.25)	11.88(10.98,12.91)	0.48(*H* value)	>0.05
Gluteus minimus *M(Q1, Q3)*	12.20(10.78,14.17)	12.31(10.96,14.59)	12.29(10.84,14.04)	0.99(*H* value)	>0.05
Iliacus *M(Q1, Q3)*	10.94(9.37,12.47)	10.86(8.79,12.21)	10.97(9.97,11.93)	3.10(*H* value)	>0.05

significant correlation between age and Young's modulus of the gluteus medius, gluteus minimus, or iliacus ($P > 0.05$).

The intra- and inter-observer evaluation results both had a high correlation (ICC = 0.855–0.933 and ICC = 0.827–0.910 respectively), and the 95% CI of both were relatively concentrated (Table 4).

Discussion

In recent years, pediatric hip diseases have received increasing attention from parents and clinicians. Developmental Dysplasia of the Hip (DDH) is the most common pediatric hip disease and bring immense pain and mental pressure to the child and their parents. At present, the diagnosis of DDH mainly relies on X-ray and ultrasound examination, while the early diagnosis before femoral head ossification mainly relies on ultrasound examination. For the treatment of DDH, the Pavlik sling is preferred for children aged 0–6 months, with regular ultrasound review; closed reduction under anesthesia and plaster tubular fixation in the herringbone position are preferred for children aged 7–18 months; closed reduction may still be attempted for children under 2 years, but most children still need open reduction and osteotomy; and children older than 8 years who have clinical symptoms need to be treated with osteotomy or hip replacement [8, 9]; therefore, it is very important to confirm the diagnosis of DDH at the earliest possible time. Therefore, it is very important to confirm the diagnosis of DDH as early as possible, when the tissue is still soft and the success rate of early treatment is greater [3]. SWE derives the value of the Young's modulus of the tissues and then quantitatively evaluates the hardness of the tissues by calculating the propagation speed of shear waves in different tissues, which plays a quantitative diagnostic role. This technique has been widely used in superficial organs such as the thyroid and breast and plays a crucial role in the diagnosis of benign and malignant diseases [10, 11]. It is also widely used in the diagnosis of musculoskeletal diseases [7, 12]. Recently, shear waves have also been reported to be used in neonatal or pediatric organs, such as the cranial brain, liver, kidney, spleen, adrenal glands and thoracic cavity [13–16], but few reports on the diagnosis of pediatric hip joints exist.

This study uses SWE technology to reflect the internal tissue structure of the hip joint and the hardness of surrounding muscles, and then obtains their normal Young's moduli to provide normal reference values for clinical practice, which can be used to distinguish between normal and pathological states of the hip joint. At the same time, it also provides theoretical support for scientific researches on the hip joint in the future.

A shear wave is a wave whose propagation direction is perpendicular to the vibration direction of the medium particles and is also known as a transverse wave. The probe emits acoustic radiation, which generates shear waves in the tissue. Through high-speed imaging technology, shear waves are acquired and then color-coded to obtain tissue elasticity images, which represent tissues of different hardnesses with different colors. Most machines are coded in blue to red, with blue representing softer tissues and red representing stiffer tissues. The shear wave propagation velocity is then calculated by the built-in analysis software in the machine to obtain the Young's modulus value of the tissue, which can quantitatively reflect the tissue hardness [17]. The hip joint consists of the femoral head and acetabulum, which are surrounded by ligaments and muscles; these structures

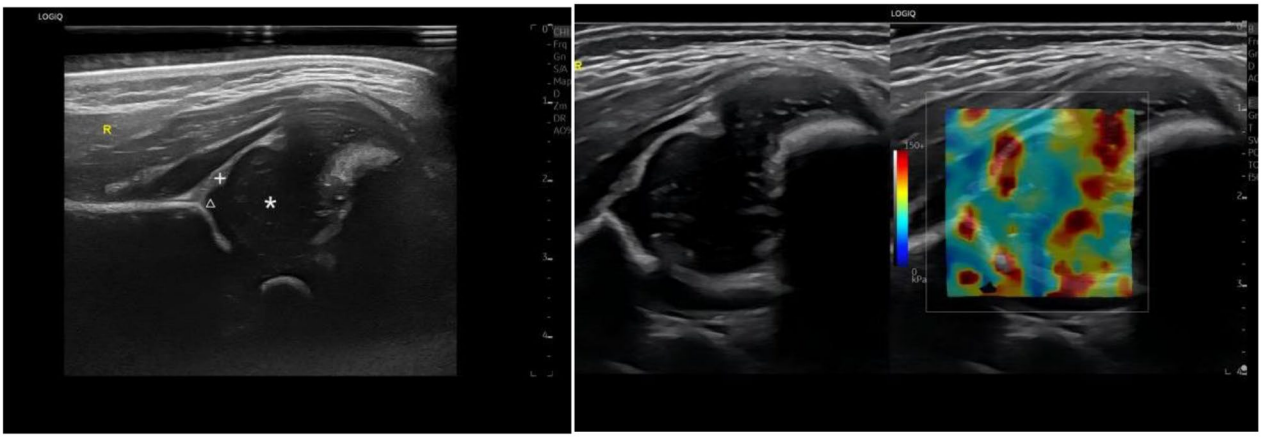

A: Grayscale image of the hip joint. B: Shear wave image of the hip joint.

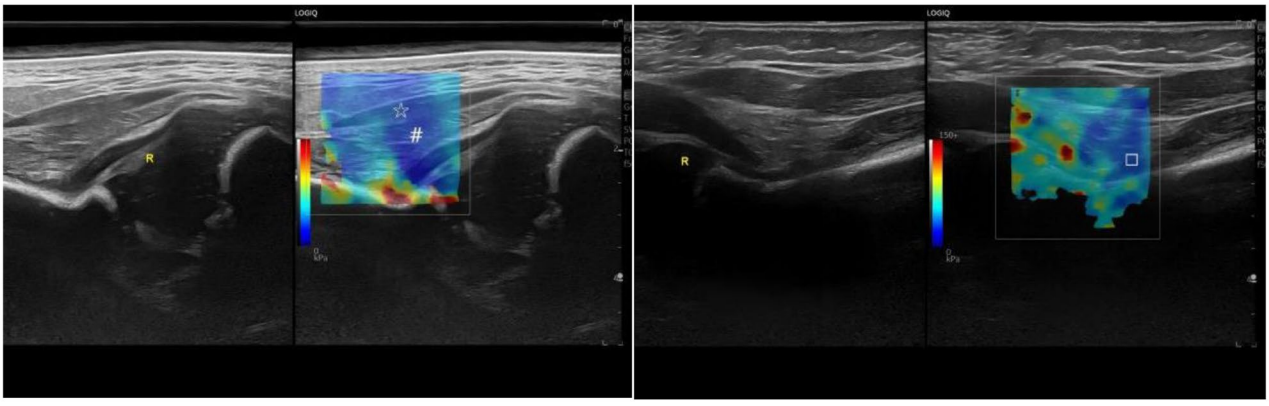

C: Shear wave images of the gluteus medius and gluteus minimus. D: Shear wave image of the iliacus.

Infant 1: Female, 2 days old. * femoral head, 16.51 kPa; +acetabular lip, 22.65 kPa; △ acetabular cartilage apex, 16.89 kPa; # gluteus minimus 14.12 kPa; ☆ gluteus medius 12.04 kPa; □ iliacus 6.79kPa.

Fig. 2 Shear wave images of various parts of the hip joint of the first group (1–30 days). *Note*: The blue to red color in the image represented that the Young's modulus was getting higher and the tissue hardness was getting harder。

have different tissue compositions, which show different colors on the elasticity image, and the Young's moduli differ accordingly. The femoral head shows a uniform blue color on the elasticity image, with Young's moduli of 23.72 ± 4.46 kPa (left) and 23.89 ± 4.41 kPa (right); this may be related to the fact that the femoral head is not ossified in the pediatric population and its composition is relatively simple, mainly consisting of cartilage, which has better sound transmission and been shown as a uniform bluish–green color on the elasticity image. The acetabular cartilage apex is composed of cartilage as the single component and has better sound transmission, and exhibits a bluish-green color similar to that of the femoral head on elasticity images, with Young's moduli of 22.47 ± 4.30 kPa (left) and 22.31 ± 4.23 kPa (right). The acetabular lip is mainly composed of cartilage and fibrous tissue. Due to its complexity of internal components relative to the femoral head and acetabular cartilage apex, the acetabular lip shows a mixed yellow–green color on elasticity images, with the corresponding Young's moduli will also increase accordingly, with 33.63 ± 6.59 kPa (left) and 33.07 ± 7.22 kPa (right), respectively. The gluteus medius, gluteus minimus and iliacus are mainly composed of muscle fibers, and the infant is in a quiet and relaxed state during the examination, so the muscle texture is relatively soft and shows a uniform blue color on the elasticity image and the Young's moduli are also correspondingly low. Whichin, the Young's moduli of the gluteus medius and iliacus are 12.09 (10.98, 13.11) kPa (left) and 11.87 (10.97, 12.95) kPa (right); those of the gluteus minimus are 11.89 (10.33, 14.05) kPa (left) and 12.39 (10.98, 14.39) kPa (right); and those of the iliacus are 10.92 (9.29, 12.19) kPa (left) and 10.98 (9.84, 12.34) kPa (right). These muscle Young's moduli are generally

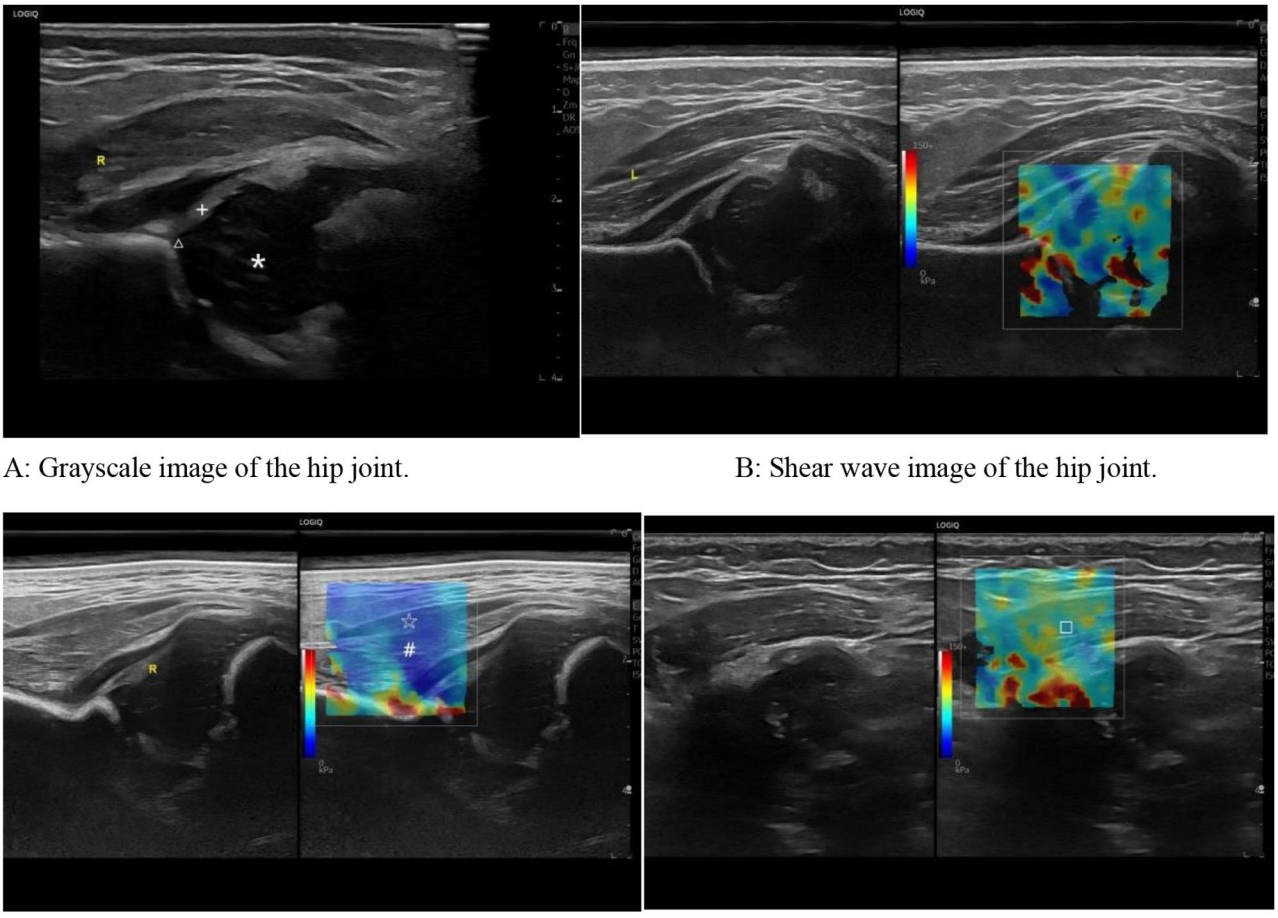

Fig. 3 Shear wave images of various parts of the hip joint of the second group (31–60 days). *Note*: The blue to red color in the image represented that the Young's modulus was getting higher and the tissue hardness was getting harder。

consistent with that mentioned in the study of Mendes B and Kato T [18, 19].

This study revealed that the differences in Young's moduli between males and females in the internal structures of the hip joint in healthy pediatric patients were not statistically significant, indicating that the SWE technique is not affected by sex in the diagnosis of hip joint diseases. A comparison between the left and right sides of each structure of the hip joints revealed no significant difference, indicating that the hardness of the tissues and structures of the bilateral hip joints of healthy pediatric patients is essentially equal. The differences in the Young's moduli of the femoral head, acetabular lip and acetabular cartilage apex of the hip joint were statistically significant and were positively correlated with age among the three groups, with the degree of tissue hardness gradually increasing with age. This is related to the gradual fibrosis and ossification of the femoral head and acetabular cartilage apex with age, which results in a gradual increase in hardness of both, the color on the elastic image gradually changes from uniform blue-green to mixed yellow-green, and the Young's moduli gradually increases. As the acetabular lip grows and develops, its fibrotic tissue and bone tissue continue to increase, making the acetabular lip harder and more firm, and further leading to an increase in its hardness. The elastic image shows a shift from yellow-green to a more yellowish color, and the Young's moduli also increase accordingly. Differences in the gluteus medius, gluteus minimus and iliacus were not statistically significant. Since ossification of the femoral head and acetabulum generally occurs between 3 and 6 months of age, ossification is not evident in infants within 3 months of age, and there is little change in Young's moduli between tissues.

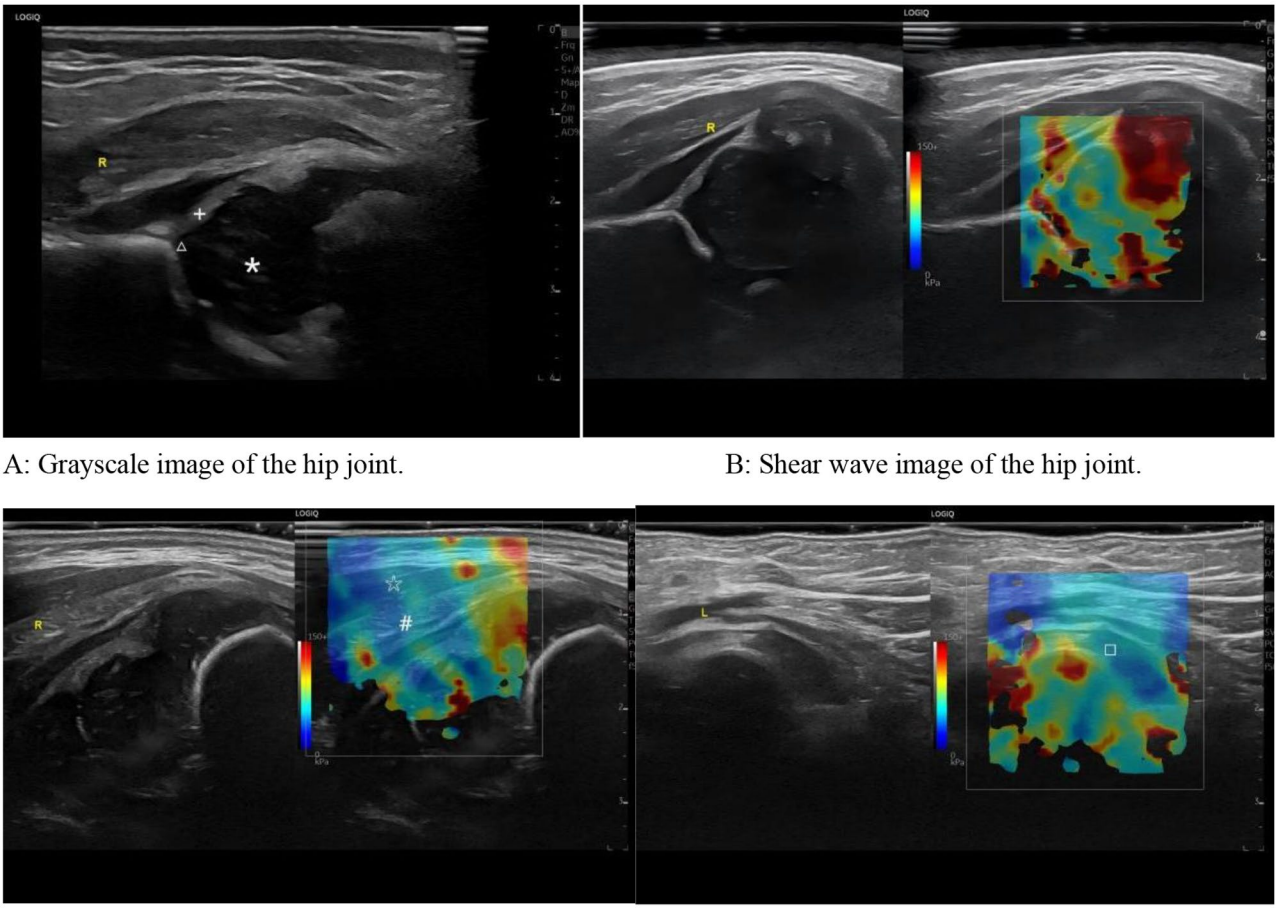

Fig. 4 Shear wave images of various parts of the hip joint of the third group (61–90 days). *Note*: The blue to red color in the image represented that the Young's modulus was getting higher and the tissue hardness was getting harder

Table 4 The intra- and inter-observer evaluation results

Groups	Intra-observer ICC (95% CI)	Inter-observer ICC (95% CI)
Femoral head	0.925 (0.909–0.938)	0.909 (0.890–0.925)
Acetabular lip	0.933 (0.919–0.945)	0.900 (0.879–0.917)
Acetabular cartilage apex	0.880 (0.55–0.901)	0.879 (0.854–0.900)
Gluteus medius	0.952 (0.942–0.961)	0.853 (0.822–0.878)
Gluteus minimus	0.855 (0.825–0.880)	0.827 (0.792–0.856)
Iliacus	0.929 (0.914–0.942)	0.910 (0.891–0.926)

Limitations

Due to the limited sample size, there may be some bias in the selection. No study has been conducted on healthy pediatric hip joint elasticity at different ages. No study has investigated whether there are differences in the Young's moduli of abnormal hip joints in pediatric patients. Data on hip elasticity in children under sedation were not studied. Future studies of large-sample data combined with artificial intelligence in children's SWE techniques for different age groups or abnormal hip joints are expected.

Conclusion

In summary, this study measured the range of Young's moduli of the femoral head, acetabular lip, acetabular cartilage apex, gluteus medius, gluteus minimus, and iliacus in the hip joint via the SWE technique, which provides a reference range of normal values in the clinic and provides a theoretical basis for subsequent research on diseases of the pediatric hip joint.

Abbreviations

SWE	Shear wave elastography
PACS	Picture Archiving and Communication System
ICC	Intraclass correlation coefficient

95% CI 95% Confidence Interval
DDH Developmental Dysplasia of the Hip

Acknowledgements
Not applicable for this section.

Author contributions
Each author has made substantial contributions to the design of the work asfollows.Fan Xiangyang: Conceptualization, Methodology, Software, Formal Analysis, Writing Original Draft; Wang Ziwei: Methodology, Data collection, Data filtering, Data analysis; Zhou Jingjing: Methodology, Software, Data analysis, Writing Original Draft; Di Min: Methodology, Data collection, Data filtering, Data analysis; He Xiao: Conceptualization, Methodology, Data analysis, Reviewing Original Draft.

Funding
None.

Data availability
The authors confirm that the data supporting the findings of this study are available within the article.

Declarations

Ethics approval
Every participant signed an informed consent approved by the First Affiliated Hospital of Zhengzhou University. Our study was conducted in accordance with the Declaration of Helsinki and approved by Ethics Committee of the First Affiliated Hospital of Zhengzhou University.

Clinical trial number
Not applicable.

Consent for publication
This manuscript has not been published or presented elsewhere in part or in entirety, and is not under consideration by another journal. There are no conflicts of interest to declare.

Competing interests
The authors declare no competing interests.

Received: 31 October 2024 / Accepted: 14 February 2025
Published online: 24 February 2025

References

1. Shaw BA, Segal LS. Evaluation and referral for Developmental Dysplasia of the hip in infants. Pediatrics. 2016;138(6):e20163107. https://doi.org/10.1542/peds.2016-3107.
2. Loder RT, Skopelja EN. The epidemiology and demographics of hip dysplasia. Isrn Orthop. 2014;2011(3):238607. https://doi.org/10.5402/2011/238607.
3. Sioutis S, Kolovos S, Papakonstantinou ME, Reppas L, Koulalis D, Mavrogenis AF. Developmental Dysplasia of the hip: a review. J Long Term Eff Med Implants. 2022;32(3):39–56. https://doi.org/10.1615/JLongTermEffMedImplants.2022040393.
4. O'Beirne JG, Chlapoutakis K, Alshryda S, Aydingoz U, Baumann T, Casini C, et al. International Interdisciplinary Consensus Meeting on the evaluation of Developmental Dysplasia of the hip. Ultraschall Med. 2019;40(4):454–64. https://doi.org/10.1055/a-0924-5491. English.
5. Aarvold A, Perry DC, Mavrotas J, Theologis T, Katchburian M, BSCOS DDH Consensus Group. The management of developmental dysplasia of the hip in children aged under three months: a consensus study from the British Society for Children's Orthopaedic Surgery. Bone Joint J. 2023;105–B(2):209–14. https://doi.org/10.1302/0301-620X.105B2.BJJ-2022-0893.R1.
6. Harper P, Joseph BM, Clarke NMP, Herrera-Soto J, Sankar WN, Schaeffer EK, et al. Even experts can be fooled: reliability of clinical examination for diagnosing hip dislocations in newborns. J Pediatr Orthop. 2020;40(8):408–12. https://doi.org/10.1097/BPO.0000000000001602.
7. Kato T, Taniguchi K, Kodesho T, Nakao G, Yokoyama Y, Saito Y, et al. Quantifying the shear modulus of the adductor longus muscle during hip joint motion using shear wave elastography. Sci Rep. 2023;13(1):9510. https://doi.org/10.1038/s41598-023-36698-w.
8. Ömeroglu H. Treatment of developmental dysplasia of the hip with the Pavlik harness in children under six months of age: indications, results and failures. J Child Orthop. 2018;12(4):308–16. https://doi.org/10.1302/1863-2548.12.180055.
9. Vaquero-Picado A, González-Morán G, Garay EG, Moraleda L. Developmental dysplasia of the hip: update of management. EFORT Open Rev. 2019;4(9):548–56. https://doi.org/10.1302/2058-5241.4.180019. Published 2019 Sep 17.
10. Hazem M, Zakaria OM, Daoud MYI, Al Jabr IK, AlYahya AA, Hassanein AG et al. Accuracy of shear wave elastography in characterization of thyroid nodules in children and adolescents. Insights Imaging. 2021;12(1):128. Published 2021 Sep 9. https://doi.org/10.1186/s13244-021-01074-7
11. Au FW, Ghai S, Moshonov H, Kahn H, Brennan C, Dua H, et al. Diagnostic performance of quantitative shear wave elastography in the evaluation of solid breast masses: determination of the most discriminatory parameter. AJR Am J Roentgenol. 2014;203(3):W328–36. https://doi.org/10.2214/AJR.13.11693.
12. Davis LC, Baumer TG, Bey MJ, Holsbeeck MV. Clinical utilization of shear wave elastography in the musculoskeletal system. Ultrasonography. 2019;38(1):2–12. https://doi.org/10.14366/usg.18039.
13. Dirrichs T, Meiser N, Panek A, Trepels-Kottek S, Orlikowsky T, Kuhl CK, et al. Transcranial Shear Wave Elastography of neonatal and infant brains for quantitative evaluation of increased intracranial pressure. Invest Radiol. 2019;54(11):719–27. https://doi.org/10.1097/RLI.0000000000000602.
14. Palabiyik FB, Inci E, Turkay R, Bas D. Evaluation of liver, kidney, and spleen elasticity in healthy newborns and infants using Shear Wave Elastography. J Ultrasound Med. 2017;36(10):2039–45. https://doi.org/10.1002/jum.14202.
15. Gürün E, Akdulum İ. Shear-wave elastography evaluation of adrenal glands in healthy newborns: a preliminary study. Rev Assoc Med Bras (1992). 2021;67(11):1724–8. https://doi.org/10.1590/1806-9282.20210825.
16. Bayramoğlu Z, Öztürk M, Çalışkan E, Ayyıldız H, Adaletli İ. Normative values of thymus in healthy children; stiffness by shear wave elastography. Diagn Interv Radiol. 2020;26(2):147–52. https://doi.org/10.5152/dir.2019.19344.
17. Sigrist RMS, Liau J, Kaffas AE, Chammas MC, Willmann JK. Ultrasound Elastography: review of techniques and clinical applications. Theranostics. 2017;7(5):1303–29. https://doi.org/10.7150/thno.18650. Published 2017 Mar 7.
18. Mendes B, Firmino T, Oliveira R, Neto T, Infante J, Vaz JR, et al. Hamstring stiffness pattern during contraction in healthy individuals: analysis by ultrasound-based shear wave elastography. Eur J Appl Physiol. 2018;118(11):2403–15. https://doi.org/10.1007/s00421-018-3967-z.
19. Kato T, Taniguchi K, Kikukawa D, Kodesho T, Katayose M. Effect of hip flexion angle on stiffness of the adductor longus muscle during isometric hip flexion. J Electromyogr Kinesiol. 2021;56:102493. https://doi.org/10.1016/j.jelekin.2020.102493.

Publisher's note